



Nguyen, D. H., Hill, T. L., & Lowenberg, M. H. (2023). Isola in a linear one-degree-of-freedom feedback system with actuator rate saturation. *International Journal of Mechanical System Dynamics*.  
<https://doi.org/10.1002/msd2.12079>

Publisher's PDF, also known as Version of record

License (if available):  
CC BY

Link to published version (if available):  
[10.1002/msd2.12079](https://doi.org/10.1002/msd2.12079)

[Link to publication record in Explore Bristol Research](#)  
PDF-document

This is the final published version of the article (version of record). It first appeared online via Wiley at <https://doi.org/10.1002/msd2.12079>. Please refer to any applicable terms of use of the publisher.

## University of Bristol - Explore Bristol Research

### General rights

This document is made available in accordance with publisher policies. Please cite only the published version using the reference above. Full terms of use are available:  
<http://www.bristol.ac.uk/red/research-policy/pure/user-guides/ebr-terms/>

# Isola in a linear one-degree-of-freedom feedback system with actuator rate saturation

Duc H. Nguyen  | Thomas L. Hill  | Mark H. Lowenberg 

Faculty of Engineering, University of Bristol, Bristol, UK

## Correspondence

Dr. Duc H. Nguyen, Faculty of Engineering, University of Bristol, Queen's Building, University Walk, Bristol BS8 1TR, UK.  
Email: [duc.nguyen@bristol.ac.uk](mailto:duc.nguyen@bristol.ac.uk)

## Funding information

None

## Abstract

This short communication uses numerical continuation to highlight the existence of an isola in a simple one-degree-of-freedom harmonically forced feedback system with actuator rate limiting as its only nonlinear element. It was found that the isola (1) contains only rate-limited responses, (2) merges with the main branch when the forcing amplitude is sufficiently large, and (3) includes stable solutions that create a second attractor in regions where rate limiting is not expected. Furthermore, the isola is composed of two solutions for a given forcing frequency. These solutions have the same amplitudes in the state (pitch rate) projection; however, they have distinct phases, and their amplitudes are also distinct when projected onto the integrator state in the controller. The rich dynamics observed in such a simple example underlines the impact of rate limiting on feedback systems. Specifically, the combination of feedback and rate limiting can create detrimental dynamics that is hard to predict and requires careful analysis.

## KEYWORDS

frequency response, harmonic forcing, rate saturation, isola, dynamical system

## 1 | INTRODUCTION

The existence of isolas in nonlinear harmonically forced systems has been verified mathematically<sup>1,2</sup> and experimentally.<sup>3,4</sup> For single degree-of-freedom (DOF) systems, researchers have attributed the formation of isolas to various factors, such as smooth nonlinear damping,<sup>5</sup> hysteresis,<sup>6</sup> piecewise nonlinearities,<sup>7</sup> and piecewise asymmetries,<sup>8</sup> among others. Many of these studies have derived comprehensive analytical solutions to predict the isolas' existence, although this has so far been limited to open-loop systems. Closed-loop systems with rate limiting can better reflect real-world setups, although this presents a new set of challenges to researchers. As far as the authors of the current manuscript are concerned, feedback systems with rate limiting can show complex

dynamics with bifurcations<sup>9,10</sup> and isolas,<sup>11,12</sup> although this has only been observed in unforced systems.

This short communication aims to facilitate further discussion of isolas in a more realistic setting. Specifically, we will investigate isola formation in a one-DOF system with the following features: harmonic forcing, feedback, and rate limiting. Feedback control and actuator rate saturation are common features of many real-world mechanical systems. By demonstrating the existence of isolas in a simple example with these features, we hope to highlight the possibility of encountering complex dynamics in experimental setups and encourage further studies.

Readers who are new to the topic can refer to the literature review section of Ref. 5, which provides a comprehensive summary of past and recent studies on isolas.

This is an open access article under the terms of the Creative Commons Attribution License, which permits use, distribution and reproduction in any medium, provided the original work is properly cited.

© 2023 The Authors. *International Journal of Mechanical System Dynamics* published by John Wiley & Sons Australia, Ltd on behalf of Nanjing University of Science and Technology.

## 2 | SIMULATION MODEL

Figure 1A shows the block-diagram representation of the system examined in this short communication. Starting from the right, the plant is a linear second-order system described by Equations (1) and (2). Preceding the plant is an actuator described by Equations (4) and (5) and Figure 1B. Essentially, this is a first-order lag with pole  $p_a$  and a rate-limiting term. Rate limiting is triggered whenever the demanded rate  $R_d = p_a(u_d - u)$  exceeds the maximum deflection rate  $\pm R_{\max}$ . Finally, a standard proportional-integral (PI) controller is used to control the plant (via the actuator) and match the feedback state  $x_1$  with the reference input  $r$ . In this scheme, the only nonlinear component is the piecewise rate-limiting term in Equation (4a).

$$\dot{x}_1 = a_{11}x_1 + a_{12}x_2 + b_{11}u, \quad (1)$$

$$\dot{x}_2 = a_{21}x_1 + a_{22}x_2 + b_{21}u, \quad (2)$$

$$\dot{E}_I = -x_1 + r, \quad (3)$$

$$\dot{u} = \begin{cases} R_{\max} \times \text{sgn}(R_d) & \text{if } |R_d| > R_{\max}, \quad (4a) \\ R_d & \text{otherwise,} \quad (4b) \end{cases}$$

where

$$\begin{aligned} R_d &= p_a(u_d - u) \\ &= -p_a K_p x_1 + p_a K_i E_I - p_a u + p_a K_p r. \end{aligned} \quad (5)$$

The plant chosen for the numerical demonstration is a linearized model of the F-16 fighter jet in straight-and-level flight at speed 200 m/s, sea-level altitude, 2.3° angle of attack, with the center of gravity located at 25% mean aerodynamic chord. This represents a normal flight condition, and the center of gravity position makes the aircraft statically stable. The aircraft model is reduced to second order to capture only the fast dynamics of the aircraft in the longitudinal plane (the short-period mode), resulting in two states:  $x_1$  for pitch rate in rad/s and  $x_2$  for angle of attack in rad. The input  $u$  to this plant is the all-moving tailplane (stabilator) deflection in degrees. The actuation system of the tailplane is modeled as a first-order lag with pole  $p_a = 50$  rad/s and maximum deflection rate  $R_{\max} = 40^\circ/\text{s}$ . Other parameters and their numerical values are listed in Table 1. The chosen plant and PI controller gains give conventional and stable

dynamics as shown in Figure 2, which is also indicative of an aircraft with good handling qualities. For the tailplane parameters, previous studies have shown that a first-order model with rate limiting can serve as an appropriate approximation.<sup>13,14</sup> Note that the two controller gains  $K_p$  and  $K_i$  are negative because  $b_{11}$  and  $b_{12}$  are negative due to sign convention, but this does not lead to loss of generality. Furthermore, since the reference signal  $r$

**TABLE 1** Parameters of the F-16 simulation.

	Symbol	Meaning	Unit/value
States	$x_1$	Pitch rate $q$	rad/s
	$x_2$	Angle of attack $\alpha$	rad
	$E_I$	Integrated error	rad
	$u$	Stabilator deflection	deg
Reference input	$r$	Demanded pitch rate ( $x_1$ )	°/s
Parameters	$p_a$	First-order actuator pole	50 rad/s
	$R_{\max}$	Maximum actuator movement rate	40°/s
	$K_p$	Proportional gain	-0.320 81
	$K_i$	Integrator gain	-3.182 9
	$a_{11}$	A-matrix element of the plant	-8.871 5
	$a_{12}$	A-matrix element of the plant	-2.270 4
	$a_{21}$	A-matrix element of the plant	-1.447 4
	$a_{22}$	A-matrix element of the plant	0.905 22
	$b_{11}$	B-matrix element of the plant	-0.357 47
	$b_{21}$	B-matrix element of the plant	-0.003 261 4
Others	$u_d$	Demanded stabilator deflection	°
	$R_d$	Demanded stabilator deflection rate	°/s

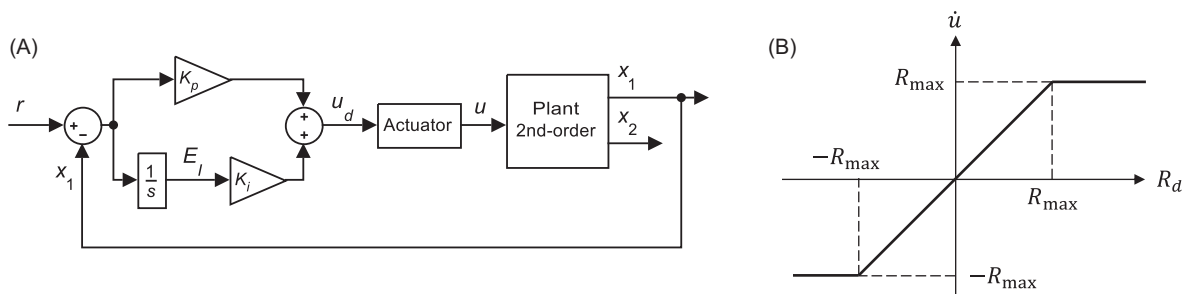


**FIGURE 1** (A) Block diagram and (B) the actuator model described by Equations (4) and (5).

(demanded pitch rate) has unit  $^{\circ}/s$ ,  $x_1$  (rad/s) in the feedback path must be multiplied by  $180/\pi$  to match the unit of the reference signal. All results are presented in SI units for convenience. Data of the full F-16 model can be found in Nguyen et al.,<sup>15</sup> and a reduced data set upon which Equations (1) and (2) were obtained can be found in the appendix of Nguyen et al.<sup>16</sup>

Regarding the relevance of the result presented, actuator rate limiting can contribute to pilot-induced oscillation, which has led to some high-profile crashes in the past.<sup>17,18</sup> The presence of an isola due to feedback and rate limiting can further exacerbate the problem, potentially leading to the dangerous “flying quality cliff” phenomenon.<sup>19</sup>

### 3 | RESULTS AND DISCUSSION

To generate the frequency response, the reference signal is now set to  $r = A \sin \omega t$ , where  $A$  ( $^{\circ}/s$ ) is the forcing amplitude,  $\omega$  (rad/s) is the forcing frequency, and  $t$  (s) is time. The resulting steady-state oscillations are calculated using the Dynamical Systems Toolbox (DST),<sup>20</sup> which is the MATLAB/Simulink implementation of the numerical continuation software AUTO-07P. The procedure of postprocessing of DST data and generation of a nonlinear Bode plot is described in Nguyen et al.<sup>21</sup>

The  $r$ -to- $x_1$  and  $r$ -to- $E_I$  Bode plots are shown in Figure 3. It can be seen that the responses are split into two families of solutions: a main

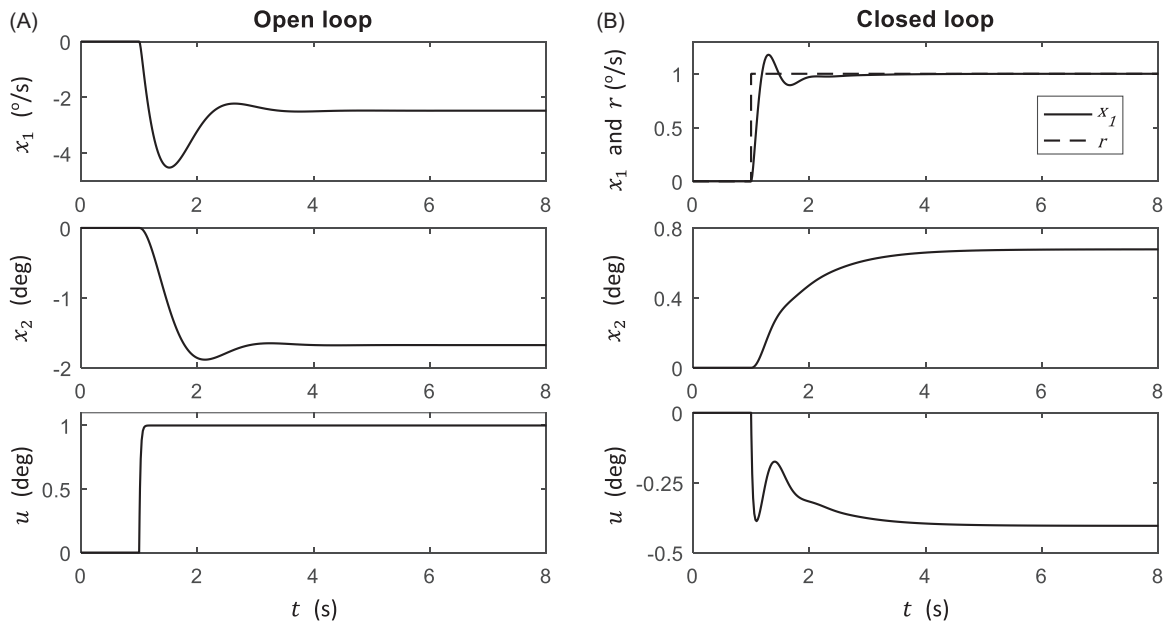


FIGURE 2 (A) Open- and (B) closed-loop step responses without rate limiting.

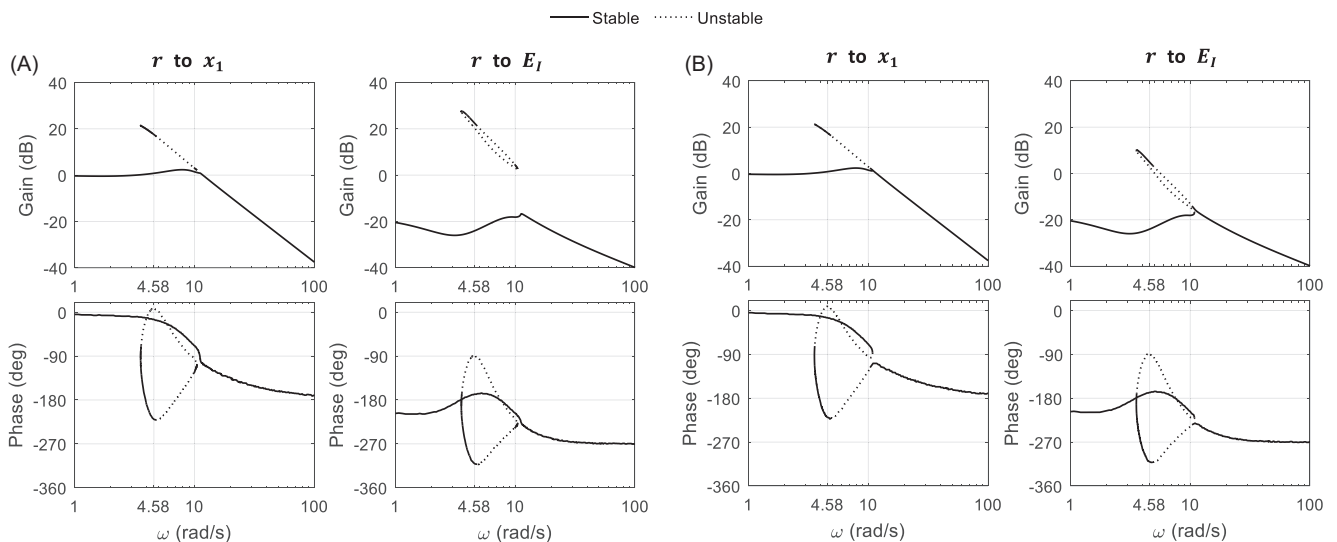


FIGURE 3 Nonlinear Bode plots at two different forcing amplitudes: (A)  $A = 7.50^{\circ}/s$  and (B)  $A = 7.57^{\circ}/s$ . Gain in dB is defined as 20 times the common logarithm of  $|x_1|/|r|$  or  $|E_I|/|r|$ .

branch covering all frequency ranges and an isola that exists between 3.55 and 10.49 rad/s. Regarding the main branch, rate limiting causes a sharper drop in both gain and phase at high frequencies compared to the linearized response (not shown). For  $A = 7.50^\circ/\text{s}$  (Figure 3A), this drop begins at around 10.2 rad/s, causing a less smooth transition in both the gain and phase plots around this frequency. Time simulations at  $\omega$  below 10.2 rad/s showed that rate limiting was not triggered as long as the response remained close to the main branch.

The isola at  $A = 7.50^\circ/\text{s}$  has three notable features:

- All solutions within the isola trigger rate limiting.
- The isola contains stable solutions near its left boundary, bounded by a fold bifurcation to the left at 3.55 rad/s and a torus bifurcation to the right at 4.82 rad/s. It is worth noting that these frequencies do not trigger rate limiting if the oscillation remains close to the main branch instead of the isola.
- For each value of  $\omega$ , all states except the integrated error  $E_I$  have two solutions with identical amplitudes but different phases.

When the forcing amplitude is increased slightly to  $A = 7.57^\circ/\text{s}$ , the isola merges with the main branch as shown in Figure 3B. Increasing  $A$  further will lead to more complex responses and eventually create a region near resonance with no stable solutions.<sup>16</sup>

The same gain but different phase features noted above is now examined. Figure 4 shows the three possible time-domain responses of the system at  $A = 7.50^\circ/\text{s}$  and  $\omega = 4.58$  rad/s. As

noted above, the stable response originating from the main branch does not trigger rate limiting and is therefore entirely linear, whereas the isola produces one stable solution and one unstable solution for each value of  $\omega$ . These two solutions cause the PI controller to create two  $E_I$  responses, and this leads to two different demanded actuator movements  $u_d$ . However, due to heavy rate saturation, the resulting two actuator responses  $u$  are of the same amplitude as the actuator cannot catch up with such a large command. The same amplitudes and different phases of the two actual actuator movements cause all physical states to have the same oscillation amplitudes and different phases, and this explains the overlapping solutions in the gain plots of the frequency responses (apart from  $E_I$ ).

Finally, the link between the isola size and the forcing amplitude  $A$  is examined. Figure 5 shows that, by reducing  $A$ , the isola becomes smaller while still retaining its overlapping-solution feature. At some point, no stable solution exists in the isola, although the existence of the unstable solutions suggests that the period-1 response can still lose stability if given a large enough perturbation. Lastly, it can be seen that reducing  $A$  to a small value of  $0.4^\circ/\text{s}$  does not eliminate the isola.

On the basis of the classification system proposed by Hirai and Sawai,<sup>22</sup> the isola projection onto  $x_1$  with overlapping solutions does not fit into any category, whereas the  $E_I$  projection suggests a more conventional "island" type. This suggests a novel type of response, which is potentially caused by the combination of feedback and rate limiting, and warrants further investigations.

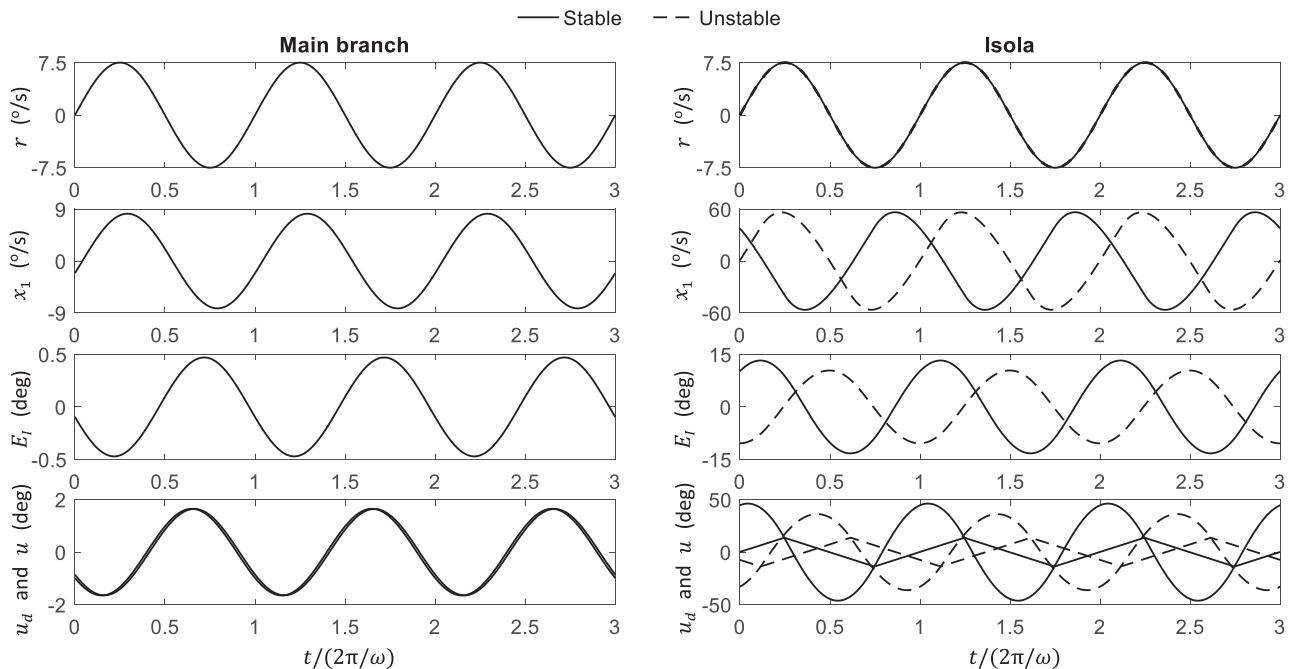


**FIGURE 4** Time-domain responses at  $A = 7.50^\circ/\text{s}$  and  $\omega = 4.58$  rad/s.

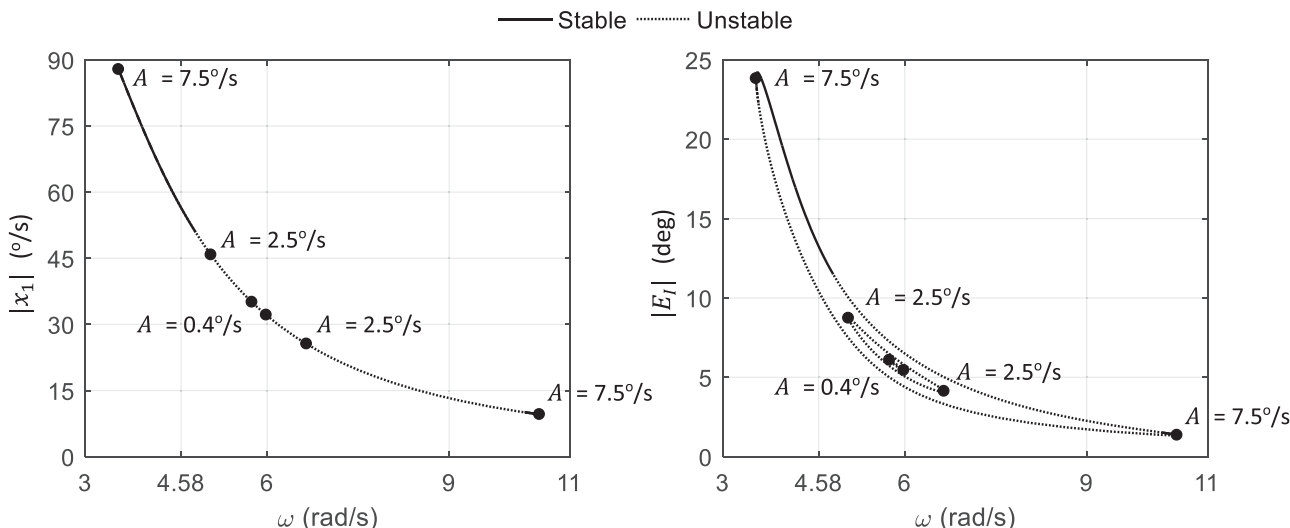


**FIGURE 5** Effect of changing the forcing amplitude  $A$  on the isola size. The large dots mark the fold bifurcations that bound the isolas at the three different values of  $A$ .

### 4 | CONCLUSIONS

This short communication has revealed the existence of isolas in a simple one-DOF system due to the combination of feedback and rate limiting. Some special features are observed, most notably the existence of two responses with the same amplitudes but different phases. The rich dynamics observed in such a simple example underlines the impact of rate limiting on the performance of feedback control, which are all-important elements of real-world mechanical systems. Further studies can consider experimental verification of the result and more rigorous mathematical treatments of the isola origin.

### CONFLICT OF INTEREST STATEMENT

The authors declare no conflict of interest.

### DATA AVAILABILITY STATEMENT

Data are sharing not applicable to this article as no data sets were generated or analyzed during the current study.

### ORCID

Duc H. Nguyen  <http://orcid.org/0000-0002-6871-7919>

Thomas L. Hill  <https://orcid.org/0000-0002-4125-7895>

Mark H. Lowenberg  <https://orcid.org/0000-0002-1373-8237>

### REFERENCES

- Hill TL, Neild SA, Cammarano A. An analytical approach for detecting isolated periodic solution branches in weakly nonlinear structures. *J Sound Vib.* 2016;379:150-165.
- Kuether RJ, Renson L, Detroux T, Grappasonni C, Kerschen G, Allen MS. Nonlinear normal modes, modal interactions and isolated resonance curves. *J Sound Vib.* 2015;351:299-310.
- Bureau E, Schilder F, Elmegård M, Santos IF, Thomsen JJ, Starke J. Experimental bifurcation analysis of an impact oscillator –determining stability. *J Sound Vib.* 2014;333(21):5464-5474.
- Renson L, Sieber J, Barton DAW, Shaw AD, Neild SA. Numerical continuation in nonlinear experiments using local Gaussian process regression. *Nonlinear Dyn.* 2019;98(4):2811-2826.
- Habib G, Cirillo GI, Kerschen G. Isolated resonances and nonlinear damping. *Nonlinear Dyn.* 2018;93(3):979-994.
- Capecchi D, Vestroni F. Periodic response of a class of hysteretic oscillators. *Int J Non-Linear Mech.* 1990;25(2):309-317.
- Duan C, Rook TE, Singh R. Sub-harmonic resonance in a nearly pre-loaded mechanical oscillator. *Nonlinear Dyn.* 2007;50(3):639-650.
- Duan C, Singh R. Isolated sub-harmonic resonance branch in the frequency response of an oscillator with slight asymmetry in the clearance. *J Sound Vib.* 2008;314(1):12-18.
- Alvarez J, Curiel LE. Bifurcations and chaos in a linear control system with saturated input. *Int J Bifurcation Chaos.* 1997;7(8):1811-1822.
- Jeffrey MR. Hidden bifurcations and attractors in nonsmooth dynamical systems. *Int J Bifurcation Chaos.* 2016;26(4):1650068.
- Andrievsky BR, Kuznetsov NV, Leonov GA, Pogromsky AY. Hidden oscillations in aircraft flight control system with input saturation. *IFAC Proc Vol.* 2013;46(12):75-79.
- Nguyen DH, Lowenberg MH, Neild SA. Identifying limits of linear control design validity in nonlinear systems: a continuation-based approach. *Nonlinear Dyn.* 2021;104(2):901-921.
- Klyde DH, McRuer DT, Myers TT. Pilot-induced oscillation analysis and prediction with actuator rate limiting. *J Guid Control Dyn.* 1997;20(1):81-89.
- Rundqwist L, Hillgren R. Phase compensation of rate limiters in JAS 39 gripen. Paper presented at: 21st Atmospheric Flight Mechanics Conference; 1996; San Diego, CA.
- Nguyen LT, Ogburn ME, Gilbert WP, Kibler KS, Brown PW, Deal PL. *Simulator Study of Stall/Post-stall Characteristics of a Fighter Airplane with Relaxed Longitudinal Static Stability.* NASA Technical 1538; 1979.
- Nguyen DH, Lowenberg MH, Neild SA. Analysing dynamic deep stall recovery using a nonlinear frequency approach. *Nonlinear Dyn.* 2022;108(2):1179-1196.

17. Orr JS, Dennehy CJ. Analysis of the X-15 flight 3-65-97 divergent limit-cycle oscillation. *J Aircr.* 2017;54(1):135-148.
18. Smith JW. *Analysis of a Longitudinal Pilot-induced Oscillation Experienced on the Approach and Landing Test of the Space Shuttle.* NASA Technical Memorandum 81366;1981.
19. McRuer DT. *Aviation Safety and Pilot Control: Understanding and Preventing Unfavorable Pilot-Vehicle Interactions.* The National Academies Press; 1997:37-46.
20. Coetzee E, Krauskopf B, Lowenberg MH. *The dynamical systems toolbox: integrating AUTO into Matlab.* Paper presented at: 16th US National Congress of Theoretical and Applied Mechanics; 27 June–2 July 2010; State College, PA.
21. Nguyen DH, Lowenberg MH, Neild SA. Frequency-domain bifurcation analysis of a nonlinear flight dynamics model. *J Guid Control Dyn.* 2021;44(1):138-150.
22. Hirai K, Sawai N. A general criterion for jump resonance of nonlinear control systems. *IEEE Trans Autom Control.* 1978;23(5):896-901.

#### AUTHOR BIOGRAPHIES



**Duc H. Nguyen** received an MEng degree in 2019 and a PhD degree in 2021 in aerospace engineering from the University of Bristol, UK. Since then, he has held both postdoctoral teaching and research roles in the Department of Aerospace Engineering at the University of Bristol. Dr. Nguyen's research experience includes flight dynamics and control, nonlinear dynamics, bifurcation methods, and automatic control of composites manufacturing. He is also a lead tutor for the University of Cambridge's online course in control engineering.



**Thomas L. Hill** received his PhD in mechanical engineering from the University of Bristol, UK, in 2015. Since 2017, he has been a lecturer in the Mechanical Engineering Department at the University of Bristol. His research interests include nonlinear reduced-order modeling, nonlinear modal interactions, and nonlinear system identification.



**Mark H. Lowenberg** has BSc and MSc Aeronautical Engineering degrees from the University of the Witwatersrand in Johannesburg and a PhD from the University of Bristol, UK. After working at the Council for Scientific & Industrial Research (CSIR) and then the University of the Witwatersrand in South Africa, he joined the University of Bristol in 1992. He has held the post of Professor of Flight Dynamics since 2014. His research interests include nonlinear problems in aerospace, especially flight dynamics and control, numerical continuation and bifurcation analysis, and novel dynamic wind tunnel test techniques.

**How to cite this article:** Nguyen DH, Hill TL, Lowenberg MH. Isola in a linear one-degree-of-freedom feedback system with actuator rate saturation. *Int J Mech Syst Dyn.* 2023;1-6.  
[doi:10.1002/msd2.12079](https://doi.org/10.1002/msd2.12079)